

A Four-Year Climatology of Total Column Tropical Urban Aerosol, Ozone and Water Vapor Distributions over Pune, India

P. C. S. Devara*, S. K. Saha, P. Ernest Raj, S. M. Sonbawne, K. K. Dani, Y. K. Tiwari, and R. S. Maheskumar

Physical Meteorology and Aerology Division, Indian Institute of Tropical Meteorology, Dr. Homi Bhabha Road, NCL Post Office, Pashan, Pune 411 008, India

Abstract

The total column aerosol optical depth, ozone and water vapor using a MICRO-processor based Total Ozone Portable Spectrometer (MICROTOPS II) and its sun photometer version have been routinely measured at the Indian Institute of Tropical Meteorology (IITM), Pune (18° 32' N, 73° 51' E, 559 m above mean sea level), India, with a view to establish an aerosol climatology over this fast growing tropical urban station. This paper focuses on spectral-temporal variations, inter-annual variability and long-term trends in the above aerosol and pre-cursor gas distributions over Pune. Besides a strong wavelength dependence of aerosol optical depth (AOD), the radiometer derived total column ozone values are found to correlate well with those estimated from the NASA's Earth Probe, Total Ozone Mapping Spectrometer (TOMS) satellite observations during the study period. The results also indicate a decreasing trend in all the above parameters, possibly due to absorbing anthropogenic aerosols during the study period, and lower Angstrom exponent, implying the prevalence of coarse-mode aerosol particles, originating from marine air mass, from around May to July, which is consistent with the ratio between the optical depths measured at 1020 and 380 nm.

Keywords: Aerosols and gases, multi-channel solar radiometer, optical extinction, climatological trends, urbanization.

1. Introduction

There has been mounting evidence of the importance of both natural and anthropogenic aerosols, particularly in the context of climate change, through their influence on formation of clouds, their effect on minor species concentration and their potential to scatter and absorb incoming solar radiation (Charlson et al. 1992). Radiative forcing due to atmospheric aerosols, particularly over

* Corresponding author. Tel: +91-020-25893600 ext. 251; Fax: +91-020-25893825.

E-mail address: devara@tropmet.res.in

tropics, is recognized to be one of the largest sources of uncertainties in assessing future global climate change (Hansen et al. 2000). The degree of confidence in estimates of aerosol radiative forcing is low due, in part, to a paucity of data on anthropogenic aerosols and hence regular monitoring of aerosols and gases is highly essential.

A wide variety of aerosol, ozone and water vapor products have been routinely measured using a ground-based, multi-filter (covering from UV to NIR wavelength region) solar radiometers at the Indian Institute of Tropical Meteorology (IITM), Pune (Lat. 18° 32' N, Long. 73° 51' E, Altitude 559 m), India. These products include column-integrated aerosol optical depth (AOD), size distribution (ASD), ozone (TCO) and precipitable water content (PWC). In this communication, we present the results of the synthesis of this extensive database, focusing on the long-term trends in the spectral-temporal variations in AOD, TCO and PWC. We also present the inter-annual variability of these parameters with a particular emphasis on the winter (urban / continental environment) and summer (maritime environment) monsoon periods since aerosols over this experimental station behave altogether differently and quite interestingly during these seasons.

2. Experimental Station and Meteorology

The experimental station, Pune, is situated on the lee-side of the Western Ghats and is about 100 km inland from the west coast of India. The environment in the immediate vicinity of the station is urban, with several small industries nearby, and the possible aerosol type present over the station is a mixture of water-soluble, dust-like and soot-type aerosols. Soil dust is the major source of aerosols at the experimental station. Formation of aerosols in the accumulation-mode ($< 1 \mu\text{m}$ radius) is considered to be due to gas-to-particle conversion processes, whereas aerosols in the coarse-mode ($> 1 \mu\text{m}$ radius) are attributed mainly to wind-blown dust.

The weather at the experimental site during the pre-monsoon season (March, April, May) is very hot with mostly gusty surface winds and the dust content in the atmosphere is at a maximum. The air flow in the lower troposphere is predominantly westerly during the south-west (SW) monsoon season (June, July, August, September), which brings a large influx of moist air from the Arabian Sea. The region receives light, continuous or intermittent rain, and the atmosphere is relatively free from dust during this season. The westerly flow sets in during the post-monsoon season (October, November). The continental air masses, rich in nuclei of continental origin, pass over the region during this season. Fair-weather conditions with clear skies, light surface winds and very low humidity exist during the winter season (December, January, February). Low-level inversions during the morning and evening hours, and dust haze during the morning hours occur during this season.

3. Measurements and Methodology

The measurements presented here were made on the terrace of the Institute's building which is located at an elevation of 573 m AMSL to make the radiometers free from nearby topographic targets like tall buildings and trees etc. The instrumentation involves two compact, on-line, multi-band solar radiometers, namely, sunphotometer and ozonometer versions of the Micro-processor based Total Ozone Portable Spectrometer (MICROTOPS II), which were operated every 10-30 min from sunrise to sunset period. Both the radiometers have been operated on over 360 clear-sky days during May 1998-December 2001, and obtained 45-50 data sets covering from sunrise to sunset period, on each experimental day. One of these radiometers provides column-integrated AOD at five wavelengths of 380, 440, 500, 675 and 870 nm. The other radiometer determines TCO in Dobson units and corrects it for aerosol scattering effects using the solar light intensity recorded at 305.5, 312.5 and 320 nm, and PWC in centimeters at 940 and 1020 nm. AOD at 1020 nm is also calculated and thus obtained AODs at a total of six wavelengths from both radiometers are utilized to retrieve wavelength exponent, which is an index of aerosol size distribution. Both these radiometers were operated using a common wooden platform with a precision elevation-azimuth assembly, so as to strictly maintain synchronization between the measured parameters in all respects. Additional details of the radiometers used in the present study have been published elsewhere (Devara et al. 2001; Morys et al. 2001; Ichoku et al. 2002).

Calibration of the radiometers is very essential for obtaining reliable results. This was performed by a transfer of calibration constants from reference instruments, which were calibrated by the Langley plot technique at a noise-free high-altitude site. Apart from this, continuous monitoring of radiometer output at zero air mass (extra-terrestrial constant), which serves as calibration constant for each channel, and also inter-instrumental comparison of AOD with simultaneously operated spectroradiometer has been carried out periodically to ensure the stability and reliability of AOD, TCO and PWC.

Total optical depths were estimated at all wavelengths by applying the computerized linear regression algorithm to the plot between natural logarithm of radiometer output voltage and air mass values (Langley plot). The aerosol optical depth, τ_a in a vertical air column at wavelength λ was determined from the Beer-Bouguer-Lambert law, expressing attenuation of direct solar beam in the atmosphere, in the form

$$F(\lambda) = F_0(\lambda) \exp [-m \{ \tau_R(\lambda) + \tau_g(\lambda) + \tau_a(\lambda) \}]$$

where $F(\lambda)$ is the monochromatic solar irradiance reaching the instrument detector, $F_0(\lambda)$ is the irradiance incident on the top-of-the-atmosphere, m is optical air mass, $\tau_R(\lambda)$, $\tau_g(\lambda)$ and $\tau_a(\lambda)$ are Rayleigh, gaseous and aerosol optical depths, respectively. The atmospheric total optical depths have been estimated by means of Langley method. The slope of the regression line gives the total optical

depth. Even though the measurements are made on clear sky days, errors may be expected due to misalignment of receiver optics. Some times, high output due to invisible (but optically visible) thin cirrus clouds also may give rise to abrupt / spurious values. Such data points were detected and removed from the raw data to avoid improper weights to the derived optical depth and to reduce the scatter in the Langley plot. This has been done by applying student's t-test. Molecular optical depth was computed by using the expression of Teillet (1990). Since ozone has significant absorption in the Chappuis band (400-650 nm) ozone optical depths at the wavelengths lie in this spectral band were estimated by the method suggested by Kneizys et al. (1980). From the total optical depths, AOD is obtained by subtracting the contributions due to molecular scattering and ozone absorption.

The total column ozone (TCO), which is equivalent to thickness of pure ozone layer at standard temperature and pressure, is measured by recording the differential absorption of solar light intensity at wavelengths in the UV region (305.5 and 320 nm). The measurement at third wavelength (312.5 nm) is used to correct for particulate scattering and stray light. The columnar or height-integrated precipitable water content (expressed in cm) is obtained from the radiance measurements made at 940 nm and 1020 nm channels of the radiometer. The estimation of PWC was made by following the differential optical absorption method applied to the irradiance data archived at 940 nm (maximum absorption for water vapor) and at 1020 nm (less absorption or almost transmission for water vapor). As the hygroscopic aerosol particles grow their size (and hence their surface area) with increase in PWC, variations in PWC will have impact on AOD and hence size distribution. PWC also influences the TCO through heterogeneous chemical processes depending on local meteorological conditions. The AOD at 1020 nm is also calculated based on the extra-terrestrial radiation at that wavelength, corrected for Sun-Earth distance, and the ground-level measurement of the radiation at 1020 nm.

The wavelength dependence of AOD contains information about the physical characteristics of aerosols. According to Junge (1955), the Angstrom or wavelength exponent (α) and Angstrom extinction coefficient (β) are related as

$$\tau_a = \beta \lambda^{-\alpha}$$

where τ_a is AOD and β is extinction or Angstrom coefficient. The relationship between exponent of Angstrom extinction and the Junge size distribution is given as

$$\alpha = v-2$$

where v is the aerosol size index. Thus a plot between τ_a and λ in log-log scale, and a power-law fit to it provides both α (slope) and β (intercept).

4. Results and Discussion

We focus our analysis primarily on the spectral-temporal variations of AOD, TCO and PWC during the winter monsoon months of December-May when the air flow is primarily from the northeast direction. This is also the time period when haze layers form due to close-to-ground inversions around December-February and intense convective activity associated with intermittent dust storms around March-April are experienced over the experimental station.

4.1. Variations in AOD, TCO and PWC on Different Time Scales

The knowledge of daily variations in aerosols and their pre-cursor gases is of primary importance to air quality. Such small-scale variations, many times, help to investigate short-lived episodic events. The daily mean values together with ± 1 sigma error bars in AOD, TCO and PWC observed during May 1998-December 2001 are shown plotted in Figure 1. It may be noted here that the AOD variations recorded at the radiometer wavelength of 380 nm (representative of fine aerosol particles) and of 500 nm (representative of sub-micron aerosol particles) are only included in this figure. The representative sizes of aerosol particles at sensing wavelengths of 380 nm and 500 nm include fine and accumulation-mode ($< 1 \mu\text{m}$ radius). Coarse-mode ($> 1 \mu\text{m}$ radius) particles need sensing at longer wavelengths, which was achieved in the present paper with the remaining channels at wavelengths of 675, 870 and 1020 nm of the radiometer. The data gaps during the south-west monsoon (June-September) in the plot are due to unfavorable sky conditions, and many times due to rain during that period. A significant annual variation in all the above three parameters with maximum AOD in pre-monsoon months and relatively minimum in winter months is quite clear from the figure. The high convective activity and frequent occurrence of dust storms are responsible for the higher AODs during the pre-monsoon. Subsequently, the AOD values attain minimum due to cloud-scavenging and rain-washout processes during the monsoon and thereafter they slowly build-up during post-monsoon and winter months and becomes maximum again in summer. Thus the annual cycle goes on over this experimental station. The very high values of AOD (close to 1 and above) noticed in the present study may possibly be due to the presence of optically thin high-altitude clouds in the experimental region.

The monthly mean spectral distributions of AOD for the period from May 1998 to December 2001 are shown plotted in Figure 2. A specific wavelength dependence of AOD i.e. decrease of AOD with increase in wavelength, which is consistent with the Mie scattering theory for aerosol particles, can be clearly seen from the figure. Relatively higher AODs at 440 nm instead 380 nm in the initial portions of spectra on some typical months may be due to gas-to-particle conversion process. This aspect is more clearly seen in Figure 3, wherein the monthly mean distributions are shown separately for individual years. In all, the AOD values are maximum during the pre-monsoon months due to the reasons as explained in the previous section. Further, greater AOD values during 1999, particularly

during winter months are considered to be due to combination of large-scale circulation processes and elevated temperature inversion-caused haze layer formations.

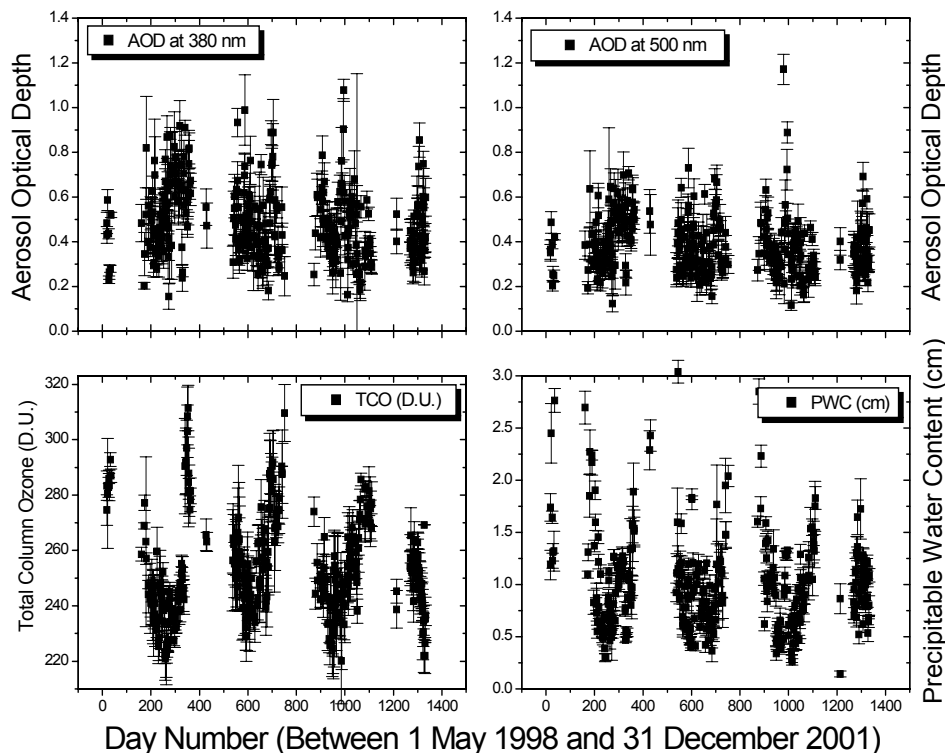


Figure 1. Daily mean variations in aerosol optical depth (AOD), total column ozone (TCO) and precipitable water content (PWC) over Pune during May 1998-December 2001. Vertical bars at each data point indicate positive and negative one sigma error.

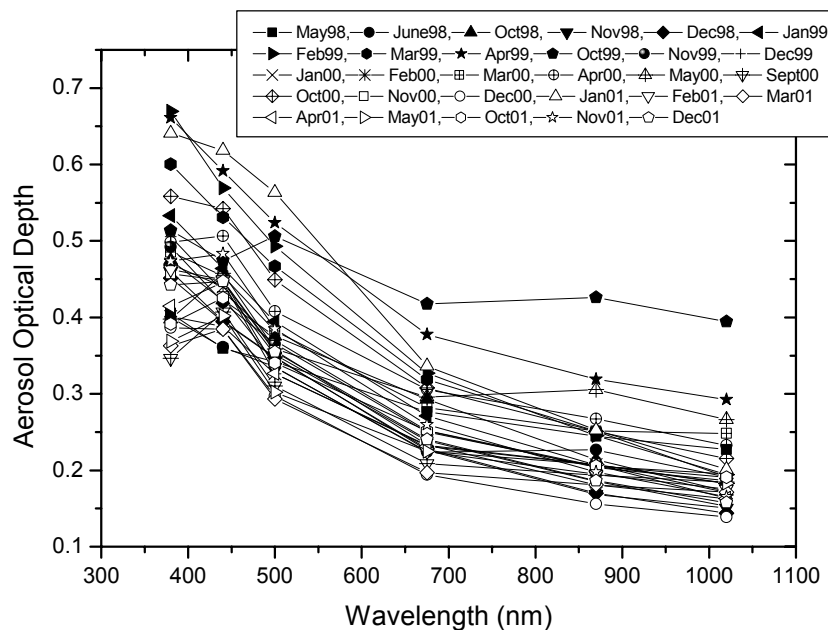


Figure 2. Monthly mean spectral distributions of AOD over Pune during May 1998-December 2001

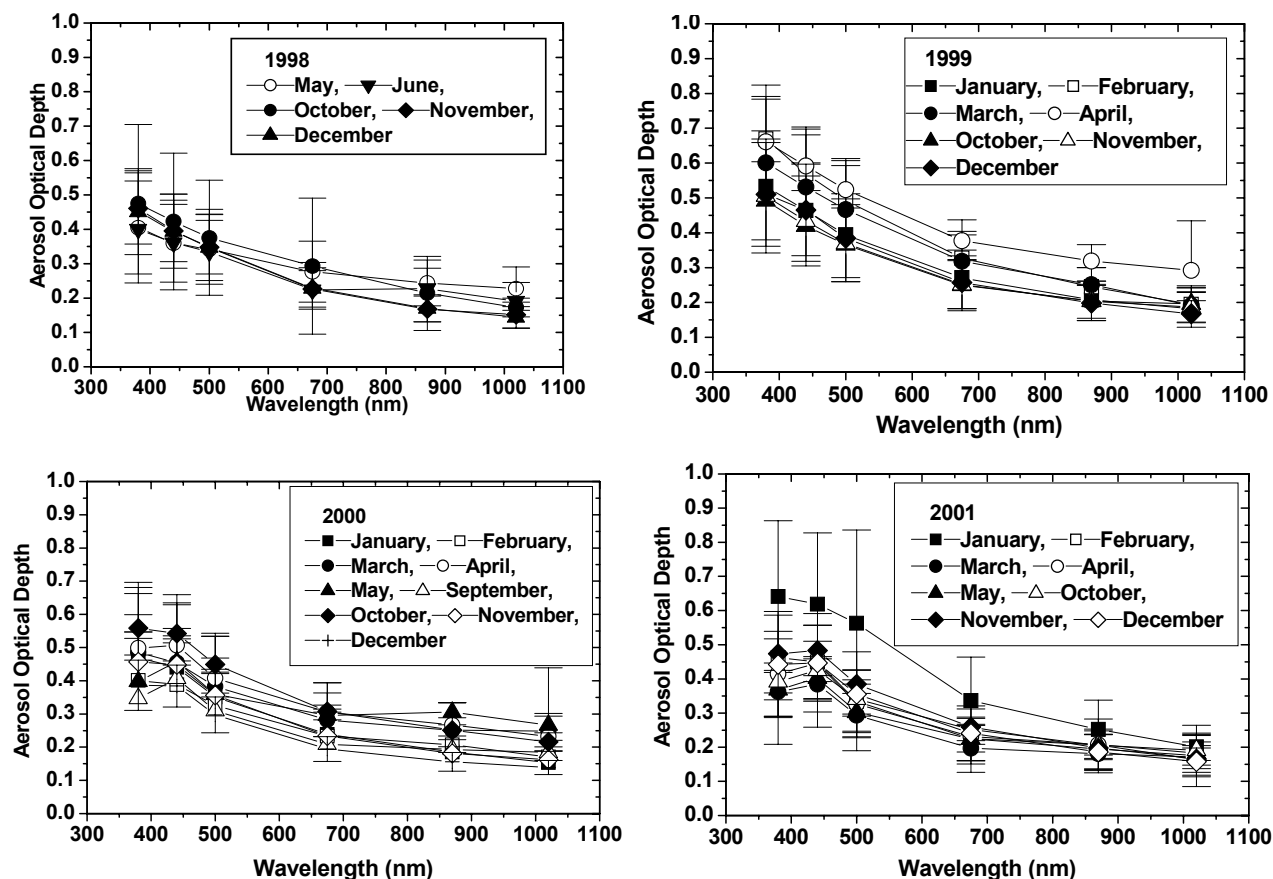


Figure 3. Wavelength dependence of aerosol optical depth during different months over Pune. Vertical lines at data points represent error bars.

4.2. Long-term Changes and Trends

The monthly mean variations in AOD, TCO and PWC during the study period are examined in Figure 4. Each value is plotted with its 1σ error bar to delineate its reliability, and errors seem to be well within the experimental limitations. In order to study the wavelength dependence, the AOD values for all the six wavelengths ranging between UV and NIR are plotted in the figure. The decrease in AOD with increase in wavelength is clearly seen from the figure, which is consistent with Mie scattering theory for aerosols. The higher values of TCO and PWC during the summer and smaller during winter months are characteristic features over this station. The dashed line in each frame that has been obtained by subjecting the data to multiple regression analysis, indicates the long-term trend in variations of the above parameters during the study period.

Besides a prominent annual cycle, as explained in Figure 1, significant inter-annual variability in AOD, TCO and PWC may be noted from Figure 4, with greater monthly average values in 1999 than those observed in 1988, 2000 and 2001, which are considered to be due to anti-cyclonic circulation that prevailed over the region during that period as reported by Srinivasan and Gadgil (2002). Another interesting feature is that all the above parameters show a decreasing trend with varying magnitude during the period of observations, which may be due to transport of greater portion of

absorbing aerosols from local as well as from neighboring regions during the period of study. The recent observations of sun/sky radiometer over this station also indicate the presence of urban-anthropogenic (absorbing) aerosols over this experimental station (Pandithurai et al., 2004). However, this aspect needs further investigation with more observations. Such studies are planned in future research as the above measurement program is continuing over this experimental station.

4.3. Variations in Angstrom Parameters

Figure 5 depicts the monthly mean values of Angstrom coefficient (β), which represents the aerosol loading and exponent (α), which represents the size distribution obtained during the study period. It is evident that the values of α and β almost opposite to each other that implies higher values of β (more extinction) are associated with smaller α (abundance of larger aerosol particles) values, which corroborate with our earlier observations over this experimental station (Mahes Kumar and Devara, 2002). Besides the usual behavior of aerosol loading (larger β value) during pre-monsoon months and relatively smaller values during winter, larger values of β and smaller values of α during winter as compared to the pre-monsoon months in certain years are attributed partly due to intense haze formation resulting from trapping of local anthropogenic aerosols, and large-scale transport of pollutants from neighboring regions over the experimental station. An interesting feature that may be worth-noting is that Angstrom exponent α exhibits lower values indicating coarse-mode aerosol particle contribution from May to July in all the four years of observations. This is possible because the marine air mass, originating from the Arabian Sea, passes over Pune during this period. In order to examine this feature further, the ratios between AODs observed at 1020 nm and 380 nm are plotted in Figure 6. This plot clearly indicates larger ratios, implying also the abundance of coarse-mode particles, particularly during the transition period from late pre-monsoon to early monsoon months.

4.4. TOMS and MICROTOPS TCO Variations

In order to investigate the compatibility between the ozone variations obtained from ground-based and satellite techniques, MICROTOPS determined TCO values are compared with TOMS derived values (Herman and Bhartia, 1997) in Figure 7. Both measurements show distinct annual oscillation with broad maximum during monsoon and minimum during winter months over this observing station. Thus, the agreement between these two techniques appears to be fairly good within the experimental limitations. The gaps during the south-west monsoon (June-September) in the case of MICROTOPS is due to cloud and precipitation hindrance to the instrument. An interesting feature is that both TOMS and MICROTOPS exhibited lower ozone values during winter and pre-monsoon months and higher values during monsoon and post-monsoon seasons of 1999. This situation is almost reverse during 2000. These changes are considered to be due to large-scale circulation induced changes in monsoon currents prevailed over the experimental region during that year.

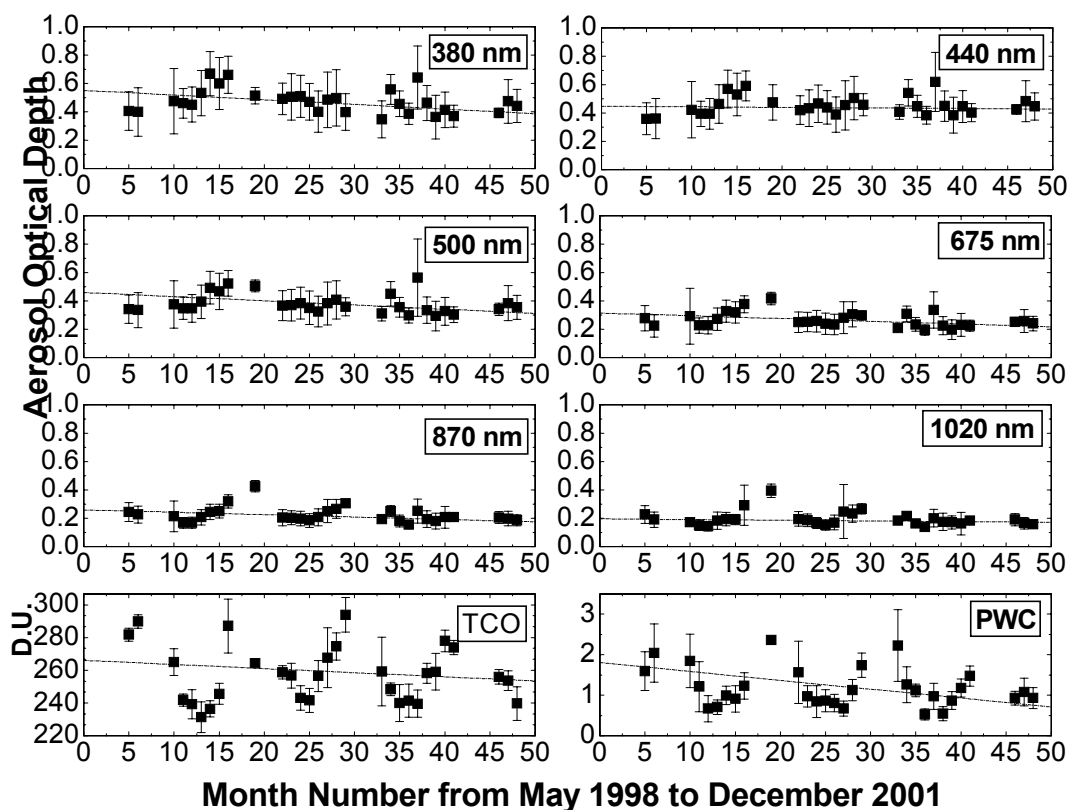


Figure 4. Long-term changes in monthly mean variations in AOD, TCO and PWC over Pune during May 1998-December 2001. The dashed line in each frame indicates trend line obtained from multiple regression analysis of data.

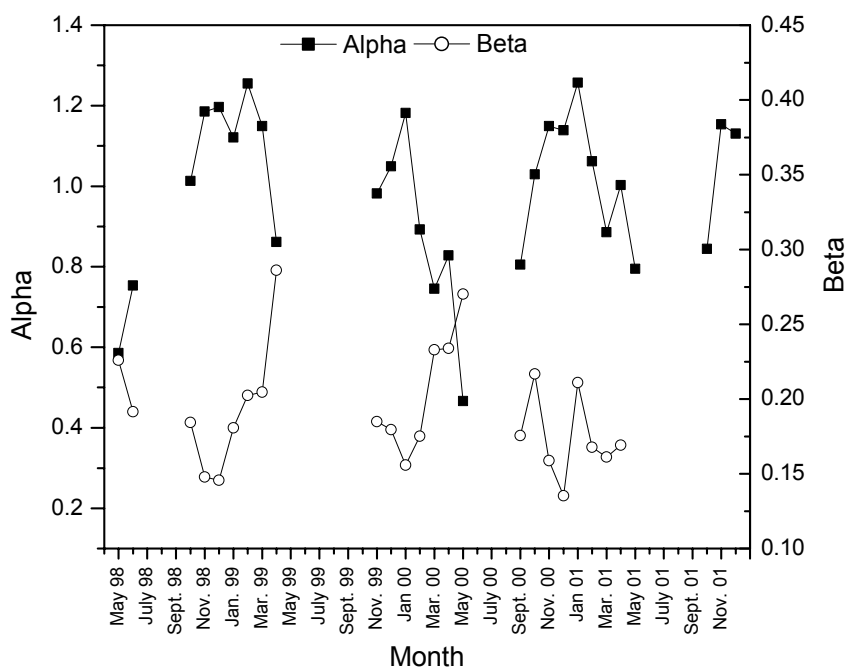


Figure 5. Monthly mean variations in Angstrom Coefficient (Beta) and Exponent (Alpha) observed over Pune during May 1998-December 2001.

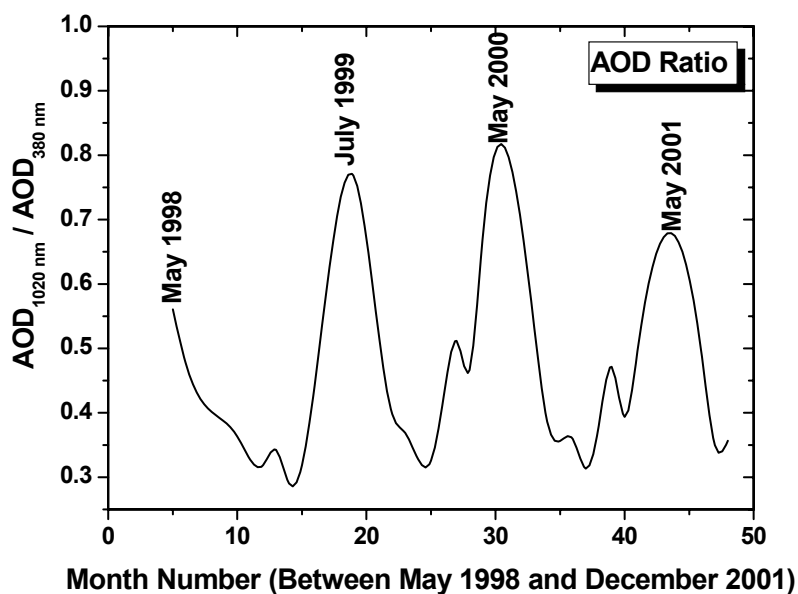


Figure 6. Monthly mean variations in ratio between AODs recorded at 1020 and 380 nm over Pune during May 1998-December 2001.

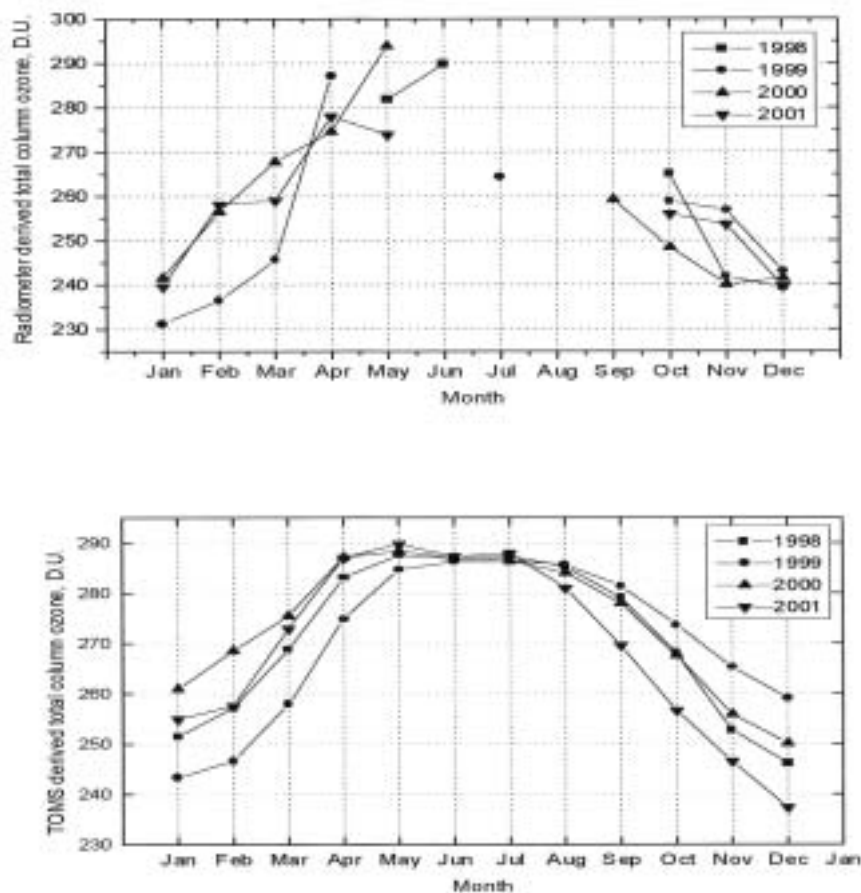


Figure 7. Comparison between total column ozone (TCO) measured by the ground-based (MICROTOPS II) radiometer and TOMS satellite over Pune during May 1998-December 2001.

5. Summary and Conclusions

A tropical urban aerosol climatology, established over Pune, India, using on-line, multi-filter solar radiometric observations carried out during May 1998-December 2001 is presented in this communication. As the observations are continuing, it is planned to update this climatology not only to understand better the features inferred from the present study but also to develop and validate models aiming at optical, physical and radiative characteristics of aerosols present over this tropical station. The chief results of the study are as follows.

(i) The column aerosol optical depth shows wavelength dependence and they exhibit larger values during pre-monsoon and relatively smaller values in winter months.

(ii) The total column aerosol optical depth, ozone and precipitable water content show decreasing trend in their variations, which is ascribed to the prevalence of absorbing aerosols at the experimental site regionally and also to the long-range transport of such aerosols from neighboring regions.

(iii) Greater Angstrom coefficient values (more loading of aerosol particles) during the pre-monsoon due to local meteorology, and some times during the winter months due to formation of elevated haze layers over Pune. Smaller Angstrom exponent values (abundance of coarse-mode aerosols originating from marine air mass) during the transition between pre-monsoon and monsoon months, which is consistent with the ratio of AODs measured at 1020 nm and 380 nm.

(iv) Radiometer-derived total column ozone values are found to correlate well with those obtained from TOMS satellite observations during the period of study.

The aerosol control strategy that one can think of from the measurements (single station) of the type reported here primarily should involve local sources as well as sources contributing from distant places through transport/circulation processes. The absorbing aerosols over urban regions originate mostly from black carbon content from diesel vehicles, fossil fuel combustion, industrial emissions and biomass/bio-fuel burning practices. Hence these practices need to be regulated to the extent that they do not affect the Earth-atmosphere radiation balance. Since the production and transformation of aerosols, both primary as well as secondary (particles forming due to gas-to-particle conversion processes), in the atmosphere depend on several parameters such as source characteristics, local meteorology, and their impact depends significantly on residence time, development of any meaningful aerosol control strategy needs three dimensional mapping of aerosol characteristics, particularly of different radiatively active gases, over longer period.

Acknowledgements

The authors wish to thank the Director, IITM for his encouragement and support. The TOMS data used for comparison in the study were obtained from the NASA website (<http://toms.gsfc.nasa.gov/eptoms>), and the same is gratefully acknowledged. The authors are also grateful to the Anonymous Reviewers for their constructive and useful comments which improved the

scientific content of the original paper.

References

- Charlson, R.J., Schwartz, S.E., Hales, J.M., Cess, R.D., Coakley, Jr., J.A., Hansen, J.E. and Hoffmann, D.J. (1992), Climate forcing by anthropogenic aerosols, *Science* 255: 423-430.
- Devara, P.C.S., Mahes Kumar, R.S., Raj, P.E., Dani, K.K. and Sonbawne, S.M. (2001), Some features of columnar aerosol optical depth, ozone and precipitable water content observed over land during the INDOEX-IFP99. *Meteorologische Zeitschrift* 10: 123-130.
- Hansen, J., Sato, M., Ruedy, R., Lacis, A. and Oinas, V. (2000), Global warming in the twenty-first century: An alternative scenario. *Proc. Natl. Acad. Sci., U.S.A.* 97: 9875-9880.
- Herman, J.R., and Bhartia, P.K. (1997), Global distribution of UV-absorbing aerosols from Nimbus 7/TOMS data. *J. Geophys. Res.* 102(D14): 16911-16922.
- Ichoku, C., Levy, R., Kaufmann, Y.J., Remer, L.A., Li, R.R., Martins, V.J., Holben, B.N., Abuhassan, N., Slutsker, I., Eck, T.F. and Pietras, C. (2002), Analysis of the performance characteristics of the five-channel Microtops II Sun photometer for measuring aerosol optical thickness and precipitable water vapour. *J. Geophys. Res.* 107(D13): 4179, doi: 10.1029/2001JD001302.
- Junge, C.E. (1955), The size distribution and aging of natural aerosols as determined from electrical and optical data on the atmosphere. *J. Meteorol.* 12: 13-25.
- Kneizys, F.X., Shettle, E.P., Gallery, W.O., Chetwynd, J.H., Abreau, L.W., Selby, J.E. A., Fenn, R. W. and McClatchey, R.A. (1980), Atmospheric Transmittance/Radiance Computer code LOWTRAN 5, AFGL-TR-80-00067. U.S. Air Force Environ Res. Paper No. 697.
- Mahes Kumar, R.S., Devara, P.C.S., Raj, P.E., Tiwari, Y.K., Pandithurai, G., Saha, S.K., Sonbawne, S. M., Dani, K.K. (2002), Synthesis of aerosol optical depth data over a tropical urban station, Proc. Conference on "Aerosol Remote Sensing in Global Change & Atmospheric Pollution" (IASTA 2002), Thiruvananthapuram, September 18-20, 2002, 27-30.
- Morys, M., Mims III, F.M., Hagerup, S., Anderson, S.E., Baker, A., Kia, J., and Walkup, T. (2001), Design, calibration and performance of MICROTOPS II handheld ozone monitor and Sun photometer. *J. Geophys. Res.* 106: 14573-14582.
- Pandithurai, G., Pinker, R.T., Takamura, T. and Devara, P.C.S. (2004), Aerosol radiative forcing over a tropical urban site in India. *Geophys. Res. Lett.* 3, L12107, doi: 10.1029/2004GL019702.
- Srinivasan, J. and Gadgil, S. (2002), Asian brown cloud - fact and fantasy. *Current Sci.* 83: 586-592.
- Teillet, P.M. (1990), Rayleigh optical depth comparison from various sources. *Appl. Opt.* 29: 1897-1900.

Received for review, February 24, 2005

Accepted, May 20, 2005